

Title

**A Comprehensive Investigation of Dog Cytochromes P450 3A (CYP3A) Reveals A Functional Role of Newly Identified CYP3A98 in Small Intestine**

Yasuhiro Uno<sup>a,\*</sup>, Shiori Jikuya<sup>a</sup>, Yutaro Noda<sup>b</sup>, Norie Murayama<sup>b</sup>, and Hiroshi Yamazaki<sup>b,\*</sup>

<sup>a</sup> Joint Faculty of Veterinary Medicine, Kagoshima University, Kagoshima-city, Kagoshima, Japan

<sup>b</sup> Laboratory of Drug Metabolism and Pharmacokinetics, Showa Pharmaceutical University, Machida, Tokyo 194-8543, Japan

**Running title:** New Dog P450 3A98 in Gut

\* All correspondence should be sent to:

1) Yasuhiro Uno, D.V.M., Ph.D.

Joint Faculty of Veterinary Medicine, Kagoshima University, 1-21-24 Korimoto, Kagoshima-city,  
Kagoshima 890-8580, Japan

Phone/Fax: +81-99-285-8715. E-mail address: unox001@vet.kagoshima-u.ac.jp

or

2) Hiroshi Yamazaki, Ph.D.

Laboratory of Drug Metabolism and Pharmacokinetics, Showa Pharmaceutical University, 3-3165  
Higashi-Tamagawa Gakuen, Machida, Tokyo 194-8543, Japan

Phone: +81-42-721-1406. Fax: +81-42-721-1406. E-mail address: hyamazak@ac.shoyaku.ac.jp

### **Abbreviations**

CYP3A, cytochromes P450 3A; P450, cytochrome P450; PCR, polymerase chain reaction; RT,  
reverse transcription; SRS, substrate recognition site.

Number of text pages: 27

Number of tables: 2

Number of figures: 9

Number of references: 33

Number of words in abstract: 250 words

Number of words in introduction: 406 words

Number of words in discussion: 1140 words

## Abstract

Dogs are frequently used in drug metabolism studies, and their important drug-metabolizing enzymes, including cytochromes P450 (P450 or CYP), have been analyzed. In humans, CYP3A4 is an especially important P450 due to its abundance and major roles in liver and intestine. In the present study, dog CYP3A98 and CYP3A99 were identified and characterized, along with previously identified CYP3A12 and CYP3A26. The dog CYP3A cDNAs contained open reading frames of 503 amino acids and shared high sequence identity (78–80%) with human CYP3As. Among the dog CYP3A mRNAs, CYP3A98 mRNA was expressed most abundantly in small intestine. In contrast, dog CYP3A12 and CYP3A26 mRNAs were expressed in liver, where CYP3A12 mRNA was the most abundant. The four *CYP3A* genes had similar gene structures and formed a gene cluster in the dog and human genomes. Metabolic assays of dog CYP3A proteins heterologously expressed in *Escherichia coli* indicated that the dog CYP3As tested were functional enzymes with respect to typical human CYP3A4 substrates. Dog CYP3A98 efficiently catalyzed oxidations of nifedipine, alprazolam, and midazolam, indicating major roles of CYP3A98 in small intestine. Dog CYP3A12 and CYP3A26 metabolizing nifedipine and/or midazolam would play roles in these reactions in liver. In contrast, dog CYP3A99 showed minimal mRNA expression and minimal metabolic activity, and its contribution to overall drug metabolism is therefore negligible. These results indicated that newly identified dog CYP3A98, a testosterone 6 $\beta$ - and estradiol 16 $\alpha$ -hydroxylase, was abundantly expressed in small intestine and is likely the major CYP3A in small intestine in combination with liver-specific CYP3A12.

### **Significance Statement**

Novel dog cytochromes P450 3A98 (CYP3A98) and CYP3A99 were identified and characterized to be functional and highly identical to human CYP3A4. Known CYP3A12 and new CYP3A98 efficiently catalyzed estradiol 16 $\alpha$ -hydroxylation and midazolam 1'-hydroxylation. CYP3A98 mRNA was expressed in small intestine, whereas CYP3A12 mRNA was predominant in liver. Dog CYP3A12 and CYP3A98, in liver and small intestine, respectively, are the enzymes likely responsible for the metabolic clearances of orally administered drugs, unlike human CYP3A4/5, which are in both liver and intestine.

## Introduction

Cytochromes P450 (P450s or CYPs) are essential drug-metabolizing enzymes in humans; of these, CYP3As are abundantly expressed in liver (Shimada et al., 1994) and metabolizes nearly half of all prescribed drugs, including nifedipine and midazolam (Wilkinson, 2005). The drug-metabolizing capability of human CYP3As vary from person to person, and this variety is partially explained by genetic polymorphisms (Zanger and Schwab, 2013). For example, protein expression of human CYP3A5 in liver varies greatly and is highly correlated with the presence of defective allele *CYP3A5\*3*; this defective allele causes aberrant splicing that generates a nonfunctional protein (Kuehl et al., 2001). The difference of abundance in CYP3As is due to ethnic differences in isoform expression, while CYP3A7 is mainly expressed in neonates (Shimada et al., 1994; Shimada et al., 1996; Zanger and Schwab, 2013).

P450s have been analyzed in dogs, a species that is frequently used as part of preclinical drug development. Two CYP3As have been identified in dogs, namely CYP3A12 (Ciaccio et al., 1991) and CYP3A26 (Fraser et al., 1997). Expression of dog CYP3A12 and CYP3A26 has been detected in liver at both the mRNA (Mealey et al., 2008; Haller et al., 2012) and protein levels, and CYP3A12 is the most abundant P450 protein in dog liver (Heikkinen et al., 2015; Martinez et al., 2019). Dog CYP3A12 and CYP3A26 are functional enzymes that metabolize human CYP3A substrates such as dextromethorphan, diazepam, and diclofenac (Shou et al., 2003; Locuson et al., 2009). Comparisons of human enzymes with those of species used in preclinical studies have shown that dogs exhibit hepatic metabolic activities toward human CYP3A substrates erythromycin and nifedipine at levels similar to those of humans, whereas cynomolgus macaques, guinea pigs, and rat enzymes show substantially greater activities (Shimada et al., 1997).

It is important to understand the roles of human CYP3A4/5 in both liver and small intestine in the metabolic clearances of orally administered drugs. In preclinical studies, to obtain some insight into the likely metabolic clearances in humans, the effects *in vitro* or *in vivo* of the responsible CYP3A enzymes in dog liver and intestine on orally administered drug candidates are investigated. In

DMD-AR-2021-000749

this study, dog genome data were analyzed, and two novel CYP3A genes (*CYP3A98* and *CYP3A99*) were identified. Their cDNAs were isolated and characterized in terms of sequence and phylogenetic analyses, gene and genomic structures, tissue expression patterns, and metabolic assays. For comparison, the two previously identified dog P450s, CYP3A12 and CYP3A26, were similarly analyzed.

## Materials and Methods

### Materials

Alprazolam, estradiol, midazolam, and testosterone were purchased from Fujifilm Wako Pure Chemicals (Osaka, Japan). Nifedipine, oxidized nifedipine, 1'-hydroxymidazolam, 4-hydroxymidazolam, 4-hydroxyalprazolam, 2-/16 $\alpha$ -hydroxyestradiol, and 6 $\beta$ -hydroxytestosterone were purchased from Sigma-Aldrich (St. Louis, MO). Pooled liver microsomes from dogs and humans were obtained from Corning Life Sciences (Woburn, MA) and intestinal microsomes were purchase from Sekisui Xenotech (Kansas City, KS). Recombinant human CYP3A4 in the bicistronic system with human NADPH-P450 reductase in bacterial membranes was prepared as described previously (Yamazaki et al., 2002). Oligonucleotides were synthesized by Integrated DNA Technologies (Coralville, IA). All other reagents were purchased from Sigma-Aldrich or Fujifilm Wako Pure Chemicals, unless otherwise specified.

### Tissues and Nucleic Acid Preparation

Dog tissue samples (adrenal gland, brain, heart, ileum, jejunum, kidney, liver, lung, and testis) were collected from a beagle dog (male, 2 years of age, weighing approximately 10 kg) at Shin Nippon Biomedical Laboratories (Kainan, Japan). From these samples, total RNA was extracted using a mirVana miRNA isolation kit (Ambion, Austin, TX) according to the manufacturer's protocols and used for cDNA cloning and the analysis of tissue expression patterns. This study was reviewed and approved by the Institutional Animal Care and Use Committee at Kagoshima University.

### Isolation of CYP3A cDNAs

Reverse transcription (RT)-polymerase chain reaction (PCR) was performed using total RNA extracted from dog liver or jejunum as previously described (Uno et al., 2006). Briefly, first-strand cDNA was synthesized in a reaction containing 1  $\mu$ g of total RNA, oligo (dT), and ReverTra Ace (TOYOBO, Osaka, Japan) at 42°C for 1 h according to the manufacturer's protocols. PCR reactions

were performed using the RT product as the template with Q5 Hot Start High-Fidelity DNA Polymerase (New England BioLabs, Ipswich, MA) in a T100 thermal cycler (Bio-Rad Laboratories, Hercules, CA) according to the manufacturer's protocols. The thermal cycler conditions were an initial denaturation at 98°C for 30 s and 35 cycles at 98°C for 10 s, 60°C for 20 s, and 72°C for 50 s, followed by a final extension at 72°C for 2 min. The primers used were dCYP3A12&26 (5rt1) 5'-GTGAAAGTACAGAGAATTCACAGAGGACGA-3' and dCYP3A12&98 (3rt1) 5'-TCTTATATCCCTACATGAGTGAAACCACATAATC-3' for CYP3A12, dCYP3A12&26 (5rt1) and dCYP3A26 (3rt1) 5'-GTCTCTGGTATTCTGGGATCCAGCTTCTTA-3' for CYP3A26, dCYP3A98 (5rt1) 5'-CTGAACAAAAGTAAAGAGAATACGCAGAAGAAAAG-3' and dCYP3A12&98 (3rt1) for CYP3A98, and dCYP3A99 (5rt1) 5'-CTGAACAAAAGTAGAGGAGACTCACAGAGAGAAAG-3' and dCYP3A99 (3rt1) 5'-GTCTGTGGTGTCTGGGATATAGCTTCTCG-3' for CYP3A99. PCR products were cloned into pMiniT2.0 vectors using a PCR Cloning Kit (New England BioLabs) according to the manufacturer's protocol. The inserts were sequenced using an ABI PRISM BigDye Terminator v3.0 Ready Reaction Cycle Sequencing Kit (Applied Biosystems, Foster City, CA) with an ABI PRISM 3500xl Genetic Analyzer (Applied Biosystems).

### Sequence Analysis

Raw sequence data were analyzed using the Genetyx system (Software Development, Tokyo, Japan), including the ClustalW program, for multiple alignment of amino acid sequences. A phylogenetic tree was created by the neighbor-joining method. BLAST (National Center for Biotechnology Information) and BLAT (UCSC Genome Bioinformatics) were used for analysis of the homology and the genome data, respectively. Amino acid and cDNA sequences used for the analyses were from GenBank or the present study.

### Measurement of mRNA Expression

Real-time RT-PCR was performed, as reported previously (Uno et al., 2006), in dog adrenal gland,



brain, heart, ileum, jejunum, kidney, liver, lung, and testis. Briefly, RT reactions were carried out using ReverTra Ace qPCR RT kit (TOYOBO) according to the manufacturer's protocols, and one-twentieth of the reaction mixture was subsequently used for PCR. PCR amplification was carried out in a total volume of 20  $\mu$ l using a THUNDERBIRD SYBR qPCR Mix Kit (TOYOBO) and a StepOnePlus Real-Time PCR System (Applied Biosystems), following the manufacturers' protocols. The following primers were used at final concentrations of 300 nM: dCYP3A12 (5qrt1) 5'-CCCAGAATTCCAAAGAAATGG-3' and dCYP3A12 (3qrt1) 5'-GGCATCGTAAGTGGGCAAT-3' for CYP3A12, dCYP3A26 (5qrt1) 5'-GTAAAGAAACACAGATCTCCCTGAGAA-3' and dCYP3A26 (3qrt1) 5'-TTCAGGTTGAATAATCCCTCGAGTA-3' for CYP3A26, dCYP3A98 (5qrt1) 5'-ATATCTGGCTCTTTCCAAAAAGTGT-3' and dCYP3A98 (3qrt1) 5'-AAATCAGATAGAGCTTTATGAGTGTCTGT-3' for CYP3A98, and dCYP3A99 (5qrt1) 5'-GAATTCTAAAGAAATGAATACCCACAA-3' and dCYP3A99 (3qrt1) 5'-AACAACAAAGATAATAGATTGAGCAACA-3' for CYP3A99. Relative expression levels were determined, based on three independent amplifications, by normalizing the raw data to the 18S ribosomal RNA level, which was measured using TaqMan Gene Expression Assays (Assay ID: Hs99999901\_s1, Applied Biosystems) with THUNDERBIRD Probe qPCR Mix (TOYOBO).

### Heterologous Protein Expression in *Escherichia coli*

Expression plasmids were generated with the CYP3A cDNAs isolated in this study, and the proteins were expressed in *Escherichia coli* DH5 $\alpha$  as reported previously (Iwata et al., 1998; Uno et al., 2006). To enhance protein expression, the *N*-terminus was modified to that of bovine CYP17, MALLLAVF (Barnes et al., 1991), by PCR-amplification of the coding region using Q5 Hot Start High-Fidelity DNA Polymerase as described earlier with the CYP3A cDNA as the template, except that the annealing step was done at 55°C. The forward primers used were dCYP3A98 (5exp1) 5'-GGAATTCCATATGGCTCTGTTATTAGCAGTTTTTATGGAAACCTGGCTTCTCCTGGCTA-3' for CYP3A98, and dCYP3A12/26/99 (5exp1)

5'-GGAATTCCATATGGCTCTGTTATTAGCAGTTTTTACAGAAACCTGGCTTCTTCTGG-3' for the remaining CYP3As. The reverse primer was dCYP3As (3exp1a) 5'-GCTCTAGAACAAAAGGGAAGTCCTTAGGGAAA for all the CYP3As. The NdeI and XbaI sites (underlined) of the forward and reverse primers, respectively, were utilized for subcloning into the pCW bicistronic vector, which contained human NADPH-P450 reductase cDNA in addition to the dog CYP3A cDNA. Protein expression using the generated expression plasmids and membrane preparations in *E.coli* were carried out as described previously (Iwata et al., 1998; Uno et al., 2006). The CYP3A protein and NADPH-P450 reductase contents in membrane preparations were determined as previously described (Phillips and Langdon, 1962; Omura and Sato, 1964; Iwata et al., 1998). Molar ratios of dog NADPH-P450 reductase/CYP3A in bacterial membranes were in the range of 4.8 to 9.2.

### Enzyme Assays

Drug oxidation activities of recombinant CYP3A enzymes and liver and small intestinal microsomes were determined for alprazolam, estradiol, midazolam, nifedipine, and testosterone as substrates using an HPLC-UV system as described previously (Uno et al., 2010; Uehara et al., 2017). Briefly, the incubation mixture consisted of 1.4–100  $\mu$ M of midazolam, 10 or 100  $\mu$ M of nifedipine or testosterone, or 20 or 200  $\mu$ M of alprazolam or estradiol; recombinant CYP3A protein (20 pmol equivalent/mL) or tissue microsomes (0.25 mg/mL); 100 mM potassium phosphate buffer (pH 7.4); and an NADPH-generating system (0.5 mM NADP<sup>+</sup>, 5 mM glucose 6-phosphate, and 1 U/mL glucose-6-phosphate dehydrogenase) in a final volume of 0.25 mL. The reaction was carried out at 37°C for 10–30 min and was terminated as described previously (Uno et al., 2010; Uehara et al., 2017).. The samples of midazolam and alprazolam were centrifuged at 2000 *g* for 5 min, and then the resulting supernatant (20–50  $\mu$ L) was injected into a reversed-phase C<sub>18</sub> column (5 mm, 250 × 4.6 mm) using isocratic elution by a mobile phase of methanol/acetonitrile/10 mM potassium phosphate buffer (pH 7.4) (24:33:43, v/v/v) at 1.5 mL/min. For nifedipine, testosterone, and estradiol oxidation, the resulting mobile phase solutions of metabolites extracted with ethyl acetate were injected into a

DMD-AR-2021-000749

reversed-phase C<sub>18</sub> column (5 mm, 150 × 4.6 mm) using isocratic elution by 64% (v/v) methanol or 33% (v/v) acetonitrile in 1% (v/v) acetic acid (for estradiol) at a flow rate of 1.0 ml/min. Kinetic parameters were calculated from a curve fitted by nonlinear regression (mean ± standard error, n = 10 substrate concentrations, in duplicate) based on the Michaelis–Menten equation (with or without substrate inhibition) using Prism (GraphPad Software, La Jolla, CA):  $v = V_{\max} \times [S]/(K_m + [S] + [S]^2/K_s)$ . One- or two-way analysis of variance was carried out using Prism (GraphPad Software, La Jolla, CA) to compare the activities among the groups.

## Results

### Identification of CYP3A cDNAs

Dog CYP3A cDNAs were successfully isolated from liver and jejunum by RT-PCR and were named by the P450 Nomenclature Committee (Nelson, 2009). These CYP3A cDNAs contained open reading frames of 503 amino acid residues with primary sequence structures characteristic of P450 proteins, such as six substrate recognition sites (SRSs) (Gotoh, 1992) and a heme-binding region (**Fig. 1**). The deduced amino acids of the CYP3As shared high sequence identity (78–80%) with human CYP3As (**Table 1**). Phylogenetic analysis of the CYP3A amino acid sequences showed that the dog enzymes were more closely related to those of humans than to those of rats (**Fig. 2**). The dog CYP3A cDNAs identified in the current study have been deposited in GenBank under the accession numbers ON164792, ON164793, ON164794, and ON164795 for CYP3A12, CYP3A26, CYP3A98, and CYP3A99, respectively.

### Genome Organization and Gene Structure of CYP3A Genes

The human and dog genomes were analyzed using BLAT to determine the genomic location of the CYP3A genes. The analysis indicated that the four CYP3A genes formed a gene cluster at corresponding locations in the dog and human genomes, but three of the genes were oriented in opposite directions in the two species (**Fig. 3**). Analysis revealed that dog and human CYP3A genes contained similar gene structures with 13 coding exons (**Fig. 4**). Dog CYP3A12, CYP3A26, CYP3A98, and CYP3A99 were approximately 35, 38, 32, and 41 kb, respectively. The sizes of the coding exons were well conserved in all the dog and human CYP3A genes, i.e., 71, 94, 53, 100, 114, 89, 149, 128, 67, 161, 227, 163, and 96 bp for exons 1–13, respectively, except for human CYP3A5 exon 12, which was 160 bp. Virtually all the dog and human CYP3A genes begin with the dinucleotide GU and end with AG, consistent with the consensus sequences for splice junctions in eukaryotic genes. These results indicated highly conserved gene structures among dog and human CYP3A genes.

### **CYP3A mRNA Expression in Tissues**

To measure the mRNA expressions of dog CYP3As, real-time RT-PCR was performed with gene-specific primers in samples of adrenal gland, brain, heart, ileum, jejunum, kidney, liver, lung, and testis. Of the tissues analyzed, dog CYP3A12 and CYP3A26 mRNAs were expressed only in liver, whereas dog CYP3A98 mRNA was predominantly expressed in jejunum and ileum (**Fig. 5**). Dog CYP3A99 mRNA was preferentially expressed in liver and small intestine (**Fig. 5**), but the expression level was minimal compared with the other three dog CYP3A mRNAs (**Fig. 6**). Among the dog CYP3A mRNAs, CYP3A12 mRNA was the most abundant in liver, followed by CYP3A26 mRNA (**Fig. 6**). In jejunum, ileum, and lung, CYP3A98 mRNA was the most abundant. In kidney, CYP3A12 mRNA was the most abundant, followed by CYP3A98 and CYP3A26 mRNAs (**Fig. 6**).

### **Drug-metabolizing Capability of CYP3A Proteins**

To determine the enzymatic properties of dog CYP3As, metabolic assays were carried out using typical human CYP3A substrates testosterone and estradiol with dog CYP3A proteins heterologously expressed in *E. coli*. Among the dog CYP3As, CYP3A98 most efficiently catalyzed testosterone 6 $\beta$ -hydroxylation (a marker reaction of human CYP3A4 in the liver microsomes) (**Fig. 7**). Dog CYP3A98 also catalyzed estradiol 16 $\alpha$ -hydroxylation (another marker reaction of human CYP3A4), along with dog CYP3A12/26, just as human CYP3A4 does (**Fig. 7**). Thus, dog CYP3A98 is a functional enzyme that contributes to the marker reactions of human CYP3A4 in dog small intestinal microsomes (**Fig. 7**).

Dog CYP3A98 was further investigated for its activity toward human CYP3A substrates nifedipine, alprazolam, and midazolam. Among the dog CYP3As, CYP3A98 most efficiently metabolized nifedipine and alprazolam, likely reflecting drug metabolism in small intestine (**Fig. 8**). CYP3A12 and CYP3A26 also metabolized nifedipine or alprazolam, thereby contributing to drug metabolism in liver (**Fig. 8**). Kinetic analyses were carried out on midazolam hydroxylation activities using recombinant dog P450 enzymes (**Fig. 9**). Dog CYP3A98 and CYP3A12 and human CYP3A4

DMD-AR-2021-000749

showed high catalytic activities at low substrate concentrations. Dog CYP3A98 and CYP3A12 catalyzed midazolam 1'-hydroxylation, a typical marker reaction of human CYP3A enzymes in liver microsomes, more efficiently than they did midazolam 4-hydroxylation, similar to the process in human liver (**Fig. 9**). The kinetic parameters calculated using the Michaelis–Menten equation with and without substrate inhibition constants are summarized in **Table 2**. Under the present conditions, dog CYP3A98 and CYP3A12 and human CYP3A4 enzymes showed low  $K_m$  values of 3.3–5.3  $\mu\text{M}$  with substrate inhibition constants ( $K_s$ ) of 72–425  $\mu\text{M}$ . The other dog P450 enzymes tested in the kinetic studies showed midazolam hydroxylation activities without  $K_s$ .

## Discussion

The current analysis of the dog genome found two new *CYP3A* gene sequences in addition to the previously identified genes *CYP3A12* and *CYP3A26*. The cDNAs of the novel *CYP3As* (*CYP3A98* and *CYP3A99*) were identified and characterized by sequence analysis, and tissue expression and metabolic assays were carried out to determine if these novel *CYP3As* are expressed and play roles as drug-metabolizing enzymes in liver and/or small intestine, which are the typical drug-metabolizing organs.

Analysis of the genome data showed that the four *CYP3A* genes formed a gene cluster at the corresponding region of the genome in dogs and humans (**Fig. 4**). Three of the genes ran in opposite directions in humans and dogs, probably as a result of differences in gene duplication event(s) that occur in each species during evolution (Nelson et al., 2004). Consequently, a one-to-one orthologous relationship of *CYP3As* was not clearly evident between the two species, despite some similarities in gene structures, tissue expression patterns, and metabolic properties.

Dog *CYP3A98* mRNA was predominantly expressed in small intestine, whereas dog *CYP3A12* and *CYP3A26* mRNAs were predominantly expressed in liver (**Fig. 5**). We found that *CYP3A12* mRNA was more abundant in liver than *CYP3A26* mRNA (**Fig. 6**). One previous study reported that *CYP3A26* mRNA was more abundant than *CYP3A12* mRNA in dog liver (Mealey et al., 2008); this inconsistency could be due to inter-individual differences, as have also been noted for human P450s (Zanger and Schwab, 2013). In other studies, *CYP3A12* was found to be more abundant at the protein level than *CYP3A26* in liver (Heikkinen et al., 2015; Martinez et al., 2019), suggesting that *CYP3A12* is likely the major *CYP3A* in dog liver. Because this study analyzed one animal for analysis of tissue expression, it is of great interest to investigate additional Beagle dogs and other dog breeds.

For small intestine, previous studies have reported that *CYP3A12* is more abundant than *CYP3A26* both in terms of mRNA (Mealey et al., 2008) and protein levels (Heikkinen et al., 2015).

However, the nucleotide and peptide sequences used to measure CYP3A12 abundance in those studies were identical to those for CYP3A98 (Uno, unpublished data); therefore, the abundance assumed to represent CYP3A12 likely reflects that of CYP3A98, considering that CYP3A98 mRNA was greatly more abundant than CYP3A12 mRNA in jejunum and ileum (**Fig. 6**). Moreover, the reported level of CYP3A12 protein decreased from the proximal to distal portion of the small intestine (Heikkinen et al., 2015), which is consistent with our finding that CYP3A98 mRNA was expressed more abundantly in jejunum than in ileum (**Fig. 5**). Therefore, CYP3A98 is likely the major CYP3A in dog small intestine.

All four dog CYP3As were functional enzymes that metabolize the human CYP3A substrates testosterone, estradiol, nifedipine, alprazolam, and midazolam (**Figs. 7-9**). Testosterone 6 $\beta$ -hydroxylation, a marker reaction of human CYP3A4, was efficiently catalyzed by CYP3A98 and CYP3A12, the latter of which likely accounts for the activity in liver microsomes because CYP3A98 is barely expressed in liver (**Fig. 7**). Testosterone 6 $\beta$ -hydroxylation activity was lower in dog liver than in human liver (**Fig. 7**), which is consistent with the findings of another study (Bogaards et al., 2000). All four dog CYP3As catalyzed both estradiol 16 $\alpha$ - and 2-hydroxylations, just as human CYP3A4 does, and this fact accounts for the activities in liver and small intestinal microsomes (**Fig. 7**). Therefore, dog CYP3As participate in the metabolism of steroids in a similar manner to that of human CYP3As.

Other human CYP3A substrates, nifedipine and alprazolam, were metabolized most efficiently by CYP3A98 among the dog CYP3As, indicating the involvement of CYP3A98 in small intestine in orally administered drug metabolism (**Fig. 8**). CYP3A12 and CYP3A26 also catalyzed this reaction, albeit with lower activities than CYP3A98, and therefore likely contribute to drug metabolism in liver (**Fig. 8**). In both dog and human liver microsomes, midazolam 1'-hydroxylation was more efficient than midazolam 4-hydroxylation (**Fig. 9**). Dog CYP3A12 and CYP3A98 efficiently catalyzed midazolam 1'-hydroxylation at comparable levels to that of human CYP3A4, indicating their involvement in this reaction in liver and small intestine, respectively (**Fig. 9, Table 2**). Other studies



have also shown the major involvement of CYP3A12 in midazolam 1'-hydroxylation and to a greater extent than CYP2B11 (Zeng et al., 2021; Wu et al., 2022), which also catalyzes this reaction (Locuson et al., 2009; Baratta et al., 2010) and is expressed in liver (Heikkinen et al., 2015; Martinez et al., 2019). CYP3A26 appears to be a minor CYP3A enzyme in dog liver because of its lower hepatic protein abundance (Heikkinen et al., 2015; Martinez et al., 2019). Therefore, midazolam 1'-hydroxylation could be a marker reaction of dog CYP3A, just as it is for human CYP3A.

The activity of dog CYP3A99 was minimal toward all the CYP3A substrates analyzed (**Figs. 7-9**), and this fact might be accounted for by amino acid substitutions of 113 residues, including 304V and 363S, compared with human CYP3A4 (**Fig. 1**). In human CYP3A4, F304 in SRS-2 is predicted to be important for binding at the active site and the substitution F304A abolishes the CYP3A4-dependent metabolism of aflatoxin B<sub>1</sub> (Xue et al., 2001). A human CYP3A4 mutant protein (T363M) is expressed at substantially lower levels by heterologous expression in bacterial membranes and shows lower catalytic activity toward testosterone 6 $\beta$ -hydroxylation (Eiselt et al., 2001; Murayama et al., 2002).

Human CYP3A4 and CYP3A5 are highly variable enzymes, partly due to genetic polymorphisms. These include *CYP3A5\*3*, a defective allele causing aberrant splicing that results in a nonfunctional protein (Kuehl et al., 2001). This allele is partly responsible for the variability of hepatic CYP3A5 expression seen in different populations, i.e., it is present in about 5–10% of Caucasians and in 60% or more of Africans or African Americans (Zanger and Schwab, 2013). Similar to humans, individual dogs and/or breeds of dogs exhibit variability in drug disposition (Hay Kraus et al., 2000; Neff et al., 2004). For dog CYP3A12, cDNA with five different amino acid residues was isolated, and the mutant protein did not affect enzyme activity for testosterone 6 $\beta$ -hydroxylation (Paulson et al., 1999). It will be important to investigate the genetic polymorphisms of dog CYP3As in the future.

In conclusion, all four dog CYP3As, including novel CYP3A98 and CYP3A99, were highly identical to human CYP3A4 and were functional enzymes that metabolize typical human CYP3A

DMD-AR-2021-000749

substrates testosterone, estradiol, nifedipine, alprazolam, and midazolam. In particular, dog CYP3A12 and CYP3A98 efficiently catalyzed marker reactions of human CYP3A, namely, testosterone 6 $\beta$ -hydroxylation, estradiol 16 $\alpha$ -hydroxylation, and midazolam 1'-hydroxylation. CYP3A98 mRNA was expressed in small intestine with the highest abundance among the four dog CYP3A mRNAs, whereas CYP3A12 mRNA was predominant in liver. Therefore, dog CYP3A12 and CYP3A98 are likely the main CYP3A enzymes in liver and small intestine, respectively, responsible for the metabolic clearances of orally administered drugs; this contrasts with the situation in humans in which CYP3A4/5 are abundantly expressed in both liver and small intestine.

## Acknowledgments

We thank Drs. Makiko Shimizu, Takanori Serizawa, and Kaito Banju for their assistance. We are also grateful to David Smallbones for copyediting a draft of this article.

### **Authorship Contributions**

*Participated in research design:* Uno and Yamazaki

*Conducted experiments:* Uno, Jikuya, Noda, and Murayama

*Contributed new reagents or analytic tools:* Uno

*Performed data analysis:* Uno and Yamazaki

*Wrote or contributed to the writing of the manuscript:* Uno and Yamazaki

## References

- Baratta MT, Zaya MJ, White JA, and Locuson CW (2010) Canine CYP2B11 metabolizes and is inhibited by anesthetic agents often co-administered in dogs. *J Vet Pharmacol Ther* **33**:50-55.
- Barnes HJ, Arlotto MP, and Waterman MR (1991) Expression and enzymatic activity of recombinant cytochrome P450 17 alpha-hydroxylase in *Escherichia coli*. *Proc Natl Acad Sci USA* **88**:5597-5601.
- Bogaards JJ, Bertrand M, Jackson P, Oudshoorn MJ, Weaver RJ, van Bladeren PJ, and Walther B (2000) Determining the best animal model for human cytochrome P450 activities: a comparison of mouse, rat, rabbit, dog, micropig, monkey and man. *Xenobiotica* **30**:1131-1152.
- Ciaccio PJ, Graves PE, Bourque DP, Glinsmann-Gibson B, and Halpert JR (1991) cDNA and deduced amino acid sequences of a dog liver cytochrome P-450 of the IIIA gene subfamily. *Biochim Biophys Acta* **1088**:319-322.
- Eiselt R, Domanski TL, Zibat A, Mueller R, Presecan-Siedel E, Hustert E, Zanger UM, Brockmoller J, Klenk HP, Meyer UA, Khan KK, He YA, Halpert JR, and Wojnowski L (2001) Identification and functional characterization of eight CYP3A4 protein variants. *Pharmacogenetics* **11**:447-458.
- Fraser DJ, Feyereisen R, Harlow GR, and Halpert JR (1997) Isolation, heterologous expression and functional characterization of a novel cytochrome P450 3A enzyme from a canine liver cDNA library. *J Pharmacol Exp Ther* **283**:1425-1432.
- Gotoh O (1992) Substrate recognition sites in cytochrome P450 family 2 (CYP2) proteins inferred from comparative analyses of amino acid and coding nucleotide sequences. *J Biol Chem* **267**:83-90.
- Haller S, Schuler F, Lazic SE, Bachir-Cherif D, Kramer SD, Parrott NJ, Steiner G, and Belli S (2012) Expression profiles of metabolic enzymes and drug transporters in the liver and along the intestine of beagle dogs. *Drug Metab Dispos* **40**:1603-1610.
- Hay Kraus BL, Greenblatt DJ, Venkatakrishnan K, and Court MH (2000) Evidence for propofol hydroxylation by cytochrome P4502B11 in canine liver microsomes: breed and gender differences. *Xenobiotica* **30**:575-588.
- Heikkinen AT, Friedlein A, Matondo M, Hatley OJ, Petsalo A, Juvonen R, Galetin A, Rostami-Hodjegan A, Aebersold R, Lamerz J, Dunkley T, Cutler P, and Parrott N (2015) Quantitative ADME proteomics – CYP and UGT enzymes in the beagle dog liver and intestine. *Pharm Res* **32**:74-90.
- Iwata H, Fujita K, Kushida H, Suzuki A, Konno Y, Nakamura K, Fujino A, and Kamataki T (1998) High catalytic activity of human cytochrome P450 co-expressed with human NADPH-cytochrome P450 reductase in *Escherichia coli*. *Biochem Pharmacol* **55**:1315-1325.

- Kuehl P, Zhang J, Lin Y, Lamba J, Assem M, Schuetz J, Watkins PB, Daly A, Wrighton SA, Hall SD, Maurel P, Relling M, Brimer C, Yasuda K, Venkataramanan R, Strom S, Thummel K, Boguski MS, and Schuetz E (2001) Sequence diversity in CYP3A promoters and characterization of the genetic basis of polymorphic CYP3A5 expression. *Nat Genet* **27**:383-391.
- Locuson CW, Ethell BT, Voice M, Lee D, and Feenstra KL (2009) Evaluation of Escherichia coli membrane preparations of canine CYP1A1, 2B11, 2C21, 2C41, 2D15, 3A12, and 3A26 with coexpressed canine cytochrome P450 reductase. *Drug Metab Dispos* **37**:457-461.
- Martinez SE, Shi J, Zhu HJ, Perez Jimenez TE, Zhu Z, and Court MH (2019) Absolute quantitation of drug-metabolizing cytochrome P450 enzymes and accessory proteins in dog liver microsomes using label-free standard-free analysis reveals interbreed variability. *Drug Metab Dispos* **47**:1314-1324.
- Mealey KL, Jabbes M, Spencer E, and Akey JM (2008) Differential expression of CYP3A12 and CYP3A26 mRNAs in canine liver and intestine. *Xenobiotica* **38**:1305-1312.
- Murayama N, Nakamura T, Saeki M, Soyama A, Saito Y, Sai K, Ishida S, Nakajima O, Itoda M, Ohno Y, Ozawa S, and Sawada J (2002) CYP3A4 gene polymorphisms influence testosterone 6beta-hydroxylation. *Drug Metab Pharmacokinet* **17**:150-156.
- Neff MW, Robertson KR, Wong AK, Safra N, Broman KW, Slatkin M, Mealey KL, and Pedersen NC (2004) Breed distribution and history of canine mdr1-1Delta, a pharmacogenetic mutation that marks the emergence of breeds from the collie lineage. *Proc Natl Acad Sci U S A* **101**:11725-11730.
- Nelson DR (2009) The cytochrome p450 homepage. *Hum Genomics* **4**:59-65.
- Nelson DR, Zeldin DC, Hoffman SM, Maltais LJ, Wain HM, and Nebert DW (2004) Comparison of cytochrome P450 (CYP) genes from the mouse and human genomes, including nomenclature recommendations for genes, pseudogenes and alternative-splice variants. *Pharmacogenetics* **14**:1-18.
- Omura T and Sato R (1964) The carbon monoxide-binding pigment of liver microsomes. I. Evidence for its hemoprotein nature. *J Biol Chem* **239**:2370-2378.
- Paulson SK, Engel L, Reitz B, Bolten S, Burton EG, Maziasz TJ, Yan B, and Schoenhard GL (1999) Evidence for polymorphism in the canine metabolism of the cyclooxygenase 2 inhibitor, celecoxib. *Drug Metab Dispos* **27**:1133-1142.
- Phillips AH and Langdon RG (1962) Hepatic triphosphopyridine nucleotide-cytochrome c reductase: isolation, characterization, and kinetic studies. *J Biol Chem* **237**:2652-2660.
- Shimada T, Mimura M, Inoue K, Nakamura S, Oda H, Ohmori S, and Yamazaki H (1997) Cytochrome P450-dependent drug oxidation activities in liver microsomes of various animal species including rats, guinea pigs, dogs, monkeys, and humans. *Arch Toxicol* **71**:401-408.
- Shimada T, Yamazaki H, Mimura M, Inui Y, and Guengerich FP (1994) Interindividual variations in

- human liver cytochrome P-450 enzymes involved in the oxidation of drugs, carcinogens and toxic chemicals: studies with liver microsomes of 30 Japanese and 30 Caucasians. *J Pharmacol Exp Ther* **270**:414-423.
- Shimada T, Yamazaki H, Mimura M, Wakamiya N, Ueng YF, Guengerich FP, and Inui Y (1996) Characterization of microsomal cytochrome P450 enzymes involved in the oxidation of xenobiotic chemicals in human fetal liver and adult lungs. *Drug Metab Dispos* **24**:515-522.
- Shou M, Norcross R, Sandig G, Lu P, Li Y, Lin Y, Mei Q, Rodrigues AD, and Rushmore TH (2003) Substrate specificity and kinetic properties of seven heterologously expressed dog cytochromes p450. *Drug Metab Dispos* **31**:1161-1169.
- Uehara S, Uno Y, Nakanishi K, Ishii S, Inoue T, Sasaki E, and Yamazaki H (2017) Marmoset cytochrome P450 3A4 ortholog expressed in liver and small-intestine tissues efficiently metabolizes midazolam, alprazolam, nifedipine, and testosterone. *Drug Metab Dispos* **45**:457-467.
- Uno Y, Fujino H, Kito G, Kamataki T, and Nagata R (2006) CYP2C76, a novel cytochrome P450 in cynomolgus monkey, is a major CYP2C in liver, metabolizing tolbutamide and testosterone. *Mol Pharmacol* **70**:477-486.
- Uno Y, Matsushita A, Osada N, Uehara S, Kohara S, Nagata R, Fukuzaki K, Utoh M, Murayama N, and Yamazaki H (2010) Genetic variants of CYP3A4 and CYP3A5 in cynomolgus and rhesus macaques. *Drug Metab Dispos* **38**:209-214.
- Wilkinson GR (2005) Drug metabolism and variability among patients in drug response. *N Engl J Med* **352**:2211-2221.
- Wu Q, Hu Y, Wang C, Wei W, Gui L, Zeng WS, Liu C, Jia W, Miao J, and Lan K (2022) Reevaluate in vitro CYP3A index reactions of benzodiazepines and steroids between humans and dogs. *Drug Metab Dispos*, in press.
- Xue L, Wang HF, Wang Q, Szklarz GD, Domanski TL, Halpert JR, and Correia MA (2001) Influence of P450 3A4 SRS-2 residues on cooperativity and/or regioselectivity of aflatoxin B(1) oxidation. *Chem Res Toxicol* **14**:483-491.
- Yamazaki H, Nakamura M, Komatsu T, Ohyama K, Hatanaka N, Asahi S, Shimada N, Guengerich FP, Shimada T, Nakajima M, and Yokoi T (2002) Roles of NADPH-P450 reductase and apo- and holo-cytochrome b5 on xenobiotic oxidations catalyzed by 12 recombinant human cytochrome P450s expressed in membranes of *Escherichia coli*. *Protein Expr Purif* **24**:329-337.
- Zanger UM and Schwab M (2013) Cytochrome P450 enzymes in drug metabolism: regulation of gene expression, enzyme activities, and impact of genetic variation. *Pharmacol Ther* **138**:103-141.
- Zeng W, Gui L, Tan X, Zhu P, Hu Y, Wu Q, Li X, Yang L, Jia W, Liu C, and Lan K (2021) Tertiary oxidation of deoxycholate is predictive of CYP3A activity in dogs. *Drug Metab Dispos* **49**:369-378.





## **Footnotes**

## **Funding**

This work was supported partly by the Japan Society for the Promotion of Science Grant-in-Aid for Scientific Research 20K06434.

## **Declaration of Interest**

The authors have no interests to declare.

Legends for figures

**Fig. 1.** Amino acid sequences of dog and human CYP3As. Amino acid sequences of dog (d) and human (h) CYP3As were aligned as described in *Materials and Methods*. A broken line above the sequences indicates the putative heme-binding region characteristic of P450 protein. The solid lines above the sequences indicate the six putative substrate recognition sites (SRSs). Asterisks and dots under the sequences indicate identical amino acids and conservatively changed amino acids, respectively.

**Fig. 2.** Phylogenetic tree of CYP3A amino acid sequences. The phylogenetic tree was created as described in *Materials and Methods* using CYP3A amino acid sequences from humans (h), cynomolgus macaques (mf), dogs (d), pigs (p), and rats (r). The scale bar indicates 0.1 amino acid substitutions per site for distance measurement. Chicken (ck) CYP3A37 was used as an outgroup.

**Fig. 3.** Genomic structure of *CYP3A* genes. The dog and human genomes were analyzed using BLAT. Four *CYP3A* genes formed gene clusters at corresponding regions in the dog and human genomes, but three of the dog *CYP3A* genes ran in opposite directions, compared to the human *CYP3A* genes. The sizes of the genes and the distances between the genes are not proportional to actual measurements.

**Fig. 4.** Gene structures of *CYP3A* genes. The coding region of each *CYP3A* cDNA sequence was aligned with the genome using BLAT to determine the gene structure of dog (d) and human (h) *CYP3A* genes.

**Fig. 5.** Tissue expression patterns of *CYP3A* mRNAs. Expression levels of dog *CYP3A* mRNAs were measured by real-time RT-PCR using gene-specific primers and probes in samples of adrenal gland, brain, heart, ileum, jejunum, kidney, liver, lung, and testis. Expression levels of each *CYP3A* mRNA were normalized to the 18S rRNA level and represent the average  $\pm$  S.D. from three independent amplifications. The most abundant expression in each graph was arbitrarily adjusted to 1, and all other expression levels were adjusted accordingly.

**Fig. 6.** Expression levels of dog CYP3A mRNAs in liver, kidney, jejunum, ileum, and lung. Expression levels were compared in each tissue type using averaged quantitative values. The most abundant expression was arbitrarily adjusted to 1, with which all other values were adjusted accordingly.

**Fig. 7.** Testosterone 6 $\beta$ -hydroxylation (A, C) and estradiol 16 $\alpha$ - and 2-hydroxylation (B, D) activities by dog liver or small intestine microsomes (A, B) and recombinant dog CYP3A enzymes (C, D). Steroid oxidation activities were determined at substrate concentrations of 10 and 100  $\mu$ M testosterone and 20 and 200  $\mu$ M estradiol in triplicate determinations. Testosterone 6 $\beta$ -hydroxylation and estradiol 16 $\alpha$ - and 2-hydroxylation activities in dog (or human) liver microsomes (A, B) were higher than those in dog (or human) intestinal liver microsomes ( $p < 0.05$ , two-way analysis of variance). A new CYP3A98 had higher testosterone 6 $\beta$ -hydroxylation activities (C) than the known CYP3A12 among four dog CYP3A enzymes tested ( $p < 0.05$ , two-way analysis of variance).

**Fig. 8.** Nifedipine (A, C) and alprazolam (B, D) oxidation activities by dog liver or small intestine microsome (A, B) and recombinant dog CYP3A enzymes (C, D). Drug oxidation activities were determined at substrate concentrations of 10 and 100  $\mu$ M nifedipine and 20 and 200  $\mu$ M alprazolam in triplicate determinations. Nifedipine and alprazolam oxidation activities in dog (or human) liver microsomes (A, B) were higher than those in dog (or human) intestinal liver microsomes ( $p < 0.05$ , two-way analysis of variance). A new CYP3A98 had higher nifedipine and alprazolam oxidation activities (C, D) than the known CYP3A12 among four dog CYP3A enzymes tested ( $p < 0.05$ , two-way analysis of variance).

**Fig. 9.** Midazolam hydroxylation catalyzed by liver microsomes and recombinant dog CYP3A proteins. Midazolam 1'- and 4-hydroxylation by liver or small intestine microsomes were determined at substrate concentrations of 10 and 100  $\mu$ M in triplicate determinations (A). Midazolam hydroxylation activities in dog (or human) liver microsomes (A) were higher than those in dog (or human) intestinal liver microsomes ( $p < 0.05$ , two-way analysis of variance). Kinetic analyses were performed for 1'- (closed symbols) and 4- (open symbols) midazolam hydroxylation activities by

DMD-AR-2021-000749

recombinant CYP3A enzymes of dogs (B, CYP3A98, circles; CYP3A99, inverted triangles; CYP3A12, triangles; CYP3A26, squares; and human CYP3A4 as a reference, diamonds). The substrate-dependent velocity curves ( $n = 10$  substrate concentrations, in duplicate) were prepared by nonlinear regression analysis. Dog CYP3A98 and CYP3A12 catalyzed midazolam 1'-hydroxylation with statistically similar  $K_m$  and  $V_{max}$  values among four dog CYP3A enzymes tested (B).

Table 1

Sequence identities of dog CYP3As compared with human CYP3As.

	Human			
	CYP3A4	CYP3A5	CYP3A7	CYP3A43
	%			
Dog				
CYP3A12	<b>80</b>	78	75	73
CYP3A26	<b>78</b>	77	74	72
CYP3A98	<b>80</b>	79	76	74
CYP3A99	<b>78</b>	76	74	72

Dog CYP3A amino acid sequences were compared with human CYP3A sequences using BLAST.

Table 2

Kinetic analyses for midazolam hydroxylation by recombinant CYP3A enzymes.

P450	Midazolam hydroxylation	$K_m$ , $\mu\text{M}$	$K_s$ , $\mu\text{M}$	$V_{\max}$ , nmol/min/nmol P450	$V_{\max}/K_m$ , ml/min/nmol
3A98	1'-hydroxylation	$5.3 \pm 3.3$	$425 \pm 30$	$47 \pm 15$	8.9
	4-hydroxylation	$27 \pm 6$	N.A.	$18 \pm 2$	0.67
3A99	1'-hydroxylation	$130 \pm 120$	N.A.	$8.6 \pm 5.1$	0.05
	4-hydroxylation	$160 \pm 130$	N.A.	$8.3 \pm 4.6$	0.05
3A12	1'-hydroxylation	$3.3 \pm 1.4$	$72 \pm 34$	$63 \pm 11$	19
	4-hydroxylation	$35 \pm 8$	N.A.	$20 \pm 2$	0.57
3A26	1'-hydroxylation	$27 \pm 6$	N.A.	$2.1 \pm 0.2$	0.08
	4-hydroxylation	$25 \pm 4$	N.A.	$4.1 \pm 0.2$	0.16
Human 3A4	1'-hydroxylation	$4.0 \pm 0.9$	$185 \pm 67$	$60 \pm 5$	15
	4-hydroxylation	$52 \pm 9$	N.A.	$41 \pm 4$	0.79

N.A., not available.

Midazolam (1.4–100  $\mu\text{M}$ ) was incubated with recombinant CYP3A enzymes (40 pmol equivalent/mL) at 37°C for 15 min. Kinetic parameters were calculated from curves fitted by nonlinear regression (mean  $\pm$  standard error,  $n = 10$  substrate concentrations, in duplicate) using the substrate inhibition equation:  $v = V_{\max} \times [S]/(K_m + [S] + [S]^2/K_s)$ . Dog CYP3A98 and CYP3A12 catalyzed midazolam 1'-hydroxylation with statistically similar  $K_m$  and  $V_{\max}$  values among four dog CYP3A enzymes tested.

# Fig. 1

```

hCYP3A4 1: MALIPDLAME TWLLLAVALV LLYLYGTHSH GLFKKLGIPG PTPLPFLGNI LSYHGFCMF DMECHKYKYG VWGFYDQQP VLAITDPDMI KTVLVKECYS 100
hCYP3A5 1: MDLIPNLAVE TWLLLAVALV LLYLYGTRTH GLFKKLGIPG PTPLPFLGNV LSYRQGLWKF DTECYKYYK MWGTYEGQLP VLAITDPDVI RTVLVKECYS 100
hCYP3A7 1: MDLIPNLAVE TWLLLAVALV LLYLYGTRTH GLFKKLGIPG PTPLPFLGNA LSPRKGWTF DMECYKYYK MWGTYDQQP VLAITDPDMI KTVLVKECYS 100
hCYP3A43 1: MDLIPNFAME TWLVATSLV LLYLYGTHSH GLFKKLGIPG PTPLPFLGTI LFYLRGLWNF DRECNEKYGE MWGLYEGQQP MLVIMDPDMI KTVLVKECYS 100
dCYP3A12 1: MDLIPSFSTE TWLLLAVALV LLYLYGTYTH GIFRKLGIPI PTPLPFLVGT LGYRNGFYVF DMKCFSKYGR MWGFYDGRQP VLAITDPDMI KTVLVKECYS 100
dCYP3A26 1: MDLIPSFSTE TWLLLAVALV LLYLYGTYTH GIFRKLGIPI PTPLPFLVGT LGYRNGFYVF DMKCFSKYGR MWGFYDGRQP VLAITDPDMI KTVLVKECYS 100
dCYP3A98 1: MDLIPSFSTE TWLLLAVALV LLYLYGTYTH GIFRKLGIPI PTPLPFLVGT LGYRNGFYVF DENCFRKYGR MWGFYDGRQP VLAITDPDMI KTVLVKECYS 100
dCYP3A99 1: MDLIPSFSTE TWLLLAVALV LFYLYGTYTH GLFKKLGIPG PTPLPFLGTI LGYRNGFYVF DEKCFRKYGR MWGFYDGRQP VLAITDPDMI KTVLVKECYS 100
*.*.*.*.* *.*.*.*.* *.*.*.*.* *.*.*.*.* *.*.*.*.* *.*.*.*.* *.*.*.*.* *.*.*.*.* *.*.*.*.* *.*.*.*.* *.*.*.*.*

SRS-1
hCYP3A4 101: VFTNRRPFGP VGFPMKSAISI AEDEEWKRLR SLLSPTFTSG KLKEMVPIIA QYGDVLRNL RREAEKGPV TLKDVFGAYS MDVITSTSPG VNIDSLNHPQ 200
hCYP3A5 101: VFTNRRSLGP VGFPMKSAISL AEDEEWKRIR SLLSPTFTSG KLKEMVPIIA QYGDVLRNL RREAEKGPV TLKDVFGAYS MDVITSTSPG VNIDSLNHPQ 200
hCYP3A7 101: VFTNRRPFGP VGFPMKNAISI AEDEEWKRIR SLLSPTFTSG KLKEMVPIIA QYGDVLRNL RREAEKGPV TLKDVFGAYS MDVITSTSPG VSIDSLNHPQ 200
hCYP3A43 101: VFTNQMPPLG MGPLKSALSF AEDEEWKRIR TLLSPAFTSV KFKEMVPIIS QCGDMLVRSR RQEAENKSI NLKDFFGAYT MDVITGTLFG VNIDSLNHPQ 200
dCYP3A12 101: VFTNRRSLGP VGFPMKSAISL SEDEEWKRM R TLLSPTFTSG KLKEMVPIIG QYGDVLRNL RKEAEKGPV NLKDVFGAYS MDVITSTSPG VNIDSLNHPQ 200
dCYP3A26 101: VFTNRRSLGP VGFPMKSAISL SEDEEWKRIR TLLSPTFTSG KLKEMVPIIG QYGDVLRNL RKEAEKGPV NLKDVFGAYS MDVITSTSPG VNIDSLNHPQ 200
dCYP3A98 101: VFTNRRSFGP VGFPMKSAISL SEDEEWKRIR TLLSPTFTSG KLKEMVPIIG QYGDVLRNL RKEAEKGPV NLKDVFGAYS MDVITSTSPG VNIDSLNHPQ 200
dCYP3A99 101: VFTNRQSGP VGFPMKSAITV SEDEEWKRIR TLLSPTFTSG KLKEMVPIIG QYGDVLRNL RKEAEKGPV NLKDVFGAYS MDVITSTSPG VNIDSLNHPQ 200
*.*.*.*.* *.*.*.*.* *.*.*.*.* *.*.*.*.* *.*.*.*.* *.*.*.*.* *.*.*.*.* *.*.*.*.* *.*.*.*.* *.*.*.*.* *.*.*.*.*

SRS-2
hCYP3A4 201: DPFVNTKLL LRFDFLDPFF LSITVFPFLI PILEVLNICV FPREVTNFLR KSVKRMKESR LEDTQKHRVD FLQLMIDSQN SKETESHKAL SDLELVAQSI 300
hCYP3A5 201: DPFVNTKLL LRFDFLDPFF LSITVFPFLI PILEVLNICV FPREVTNFLR KSVKRMKESR LEDTQKHRVD FLQLMIDSQN SKETESHKAL SDLELVAQSI 300
hCYP3A7 201: DPFVNTKLL LRFDFLDPFF LSITVFPFLI PILEVLNICV FPREVTNFLR KSVKRMKESR LEDTQKHRVD FLQLMIDSQN SKETESHKAL SDLELVAQSI 300
hCYP3A43 201: DPFVNTKLL LRFDFLDPFF LSITVFPFLI PILEVLNICV FPREVTNFLR KSVKRMKESR LEDTQKHRVD FLQLMIDSQN SKETESHKAL SDLELVAQSI 300
dCYP3A12 201: DPFVNTKLL LRFDFLDPFF LSITVFPFLI PILEVLNICV FPREVTNFLR KSVKRMKESR LEDTQKHRVD FLQLMIDSQN SKETESHKAL SDLELVAQSI 300
dCYP3A26 201: DPFVNTKLL LRFDFLDPFF LSITVFPFLI PILEVLNICV FPREVTNFLR KSVKRMKESR LEDTQKHRVD FLQLMIDSQN SKETESHKAL SDLELVAQSI 300
dCYP3A98 201: DPFVNTKLL LRFDFLDPFF LSITVFPFLI PILEVLNICV FPREVTNFLR KSVKRMKESR LEDTQKHRVD FLQLMIDSQN SKETESHKAL SDLELVAQSI 300
dCYP3A99 201: DPFVNTKLL LRFDFLDPFF LSITVFPFLI PILEVLNICV FPREVTNFLR KSVKRMKESR LEDTQKHRVD FLQLMIDSQN SKETESHKAL SDLELVAQSI 300
*.*.*.*.* *.*.*.*.* *.*.*.*.* *.*.*.*.* *.*.*.*.* *.*.*.*.* *.*.*.*.* *.*.*.*.* *.*.*.*.* *.*.*.*.* *.*.*.*.*

SRS-3
hCYP3A4 201: DPFVNTKLL LRFDFLDPFF LSITVFPFLI PILEVLNICV FPREVTNFLR KSVKRMKESR LEDTQKHRVD FLQLMIDSQN SKETESHKAL SDLELVAQSI 300
hCYP3A5 201: DPFVNTKLL LRFDFLDPFF LSITVFPFLI PILEVLNICV FPREVTNFLR KSVKRMKESR LEDTQKHRVD FLQLMIDSQN SKETESHKAL SDLELVAQSI 300
hCYP3A7 201: DPFVNTKLL LRFDFLDPFF LSITVFPFLI PILEVLNICV FPREVTNFLR KSVKRMKESR LEDTQKHRVD FLQLMIDSQN SKETESHKAL SDLELVAQSI 300
hCYP3A43 201: DPFVNTKLL LRFDFLDPFF LSITVFPFLI PILEVLNICV FPREVTNFLR KSVKRMKESR LEDTQKHRVD FLQLMIDSQN SKETESHKAL SDLELVAQSI 300
dCYP3A12 201: DPFVNTKLL LRFDFLDPFF LSITVFPFLI PILEVLNICV FPREVTNFLR KSVKRMKESR LEDTQKHRVD FLQLMIDSQN SKETESHKAL SDLELVAQSI 300
dCYP3A26 201: DPFVNTKLL LRFDFLDPFF LSITVFPFLI PILEVLNICV FPREVTNFLR KSVKRMKESR LEDTQKHRVD FLQLMIDSQN SKETESHKAL SDLELVAQSI 300
dCYP3A98 201: DPFVNTKLL LRFDFLDPFF LSITVFPFLI PILEVLNICV FPREVTNFLR KSVKRMKESR LEDTQKHRVD FLQLMIDSQN SKETESHKAL SDLELVAQSI 300
dCYP3A99 201: DPFVNTKLL LRFDFLDPFF LSITVFPFLI PILEVLNICV FPREVTNFLR KSVKRMKESR LEDTQKHRVD FLQLMIDSQN SKETESHKAL SDLELVAQSI 300
*.*.*.*.* *.*.*.*.* *.*.*.*.* *.*.*.*.* *.*.*.*.* *.*.*.*.* *.*.*.*.* *.*.*.*.* *.*.*.*.* *.*.*.*.* *.*.*.*.*

SRS-4
hCYP3A4 301: IFIFAGYETT SSVLSFIMYE LATHPDVQQK LQEEIDAVLP NKAPPTYDTV LQMEYLDMMV NETLRLFPVA MRLEVRCKKD VEINGVFIPK GVVVMIPSYA 400
hCYP3A5 301: IFIFAGYETT SSVLSFIMYE LATHPDVQQK LQEEIDAVLP NKAPPTYDTV LQMEYLDMMV NETLRLFPVA MRLEVRCKKD VEINGVFIPK GVVVMIPSYA 400
hCYP3A7 301: IFIFAGYETT SSVLSFIMYE LATHPDVQQK LQEEIDAVLP NKAPPTYDTV LQMEYLDMMV NETLRLFPVA MRLEVRCKKD VEINGVFIPK GVVVMIPSYA 400
hCYP3A43 301: IFIFAGYETT SSVLSFIMYE LATHPDVQQK LQEEIDAVLP NKAPPTYDTV LQMEYLDMMV NETLRLFPVA MRLEVRCKKD VEINGVFIPK GVVVMIPSYA 400
dCYP3A12 301: IFIFAGYETT SSVLSFIMYE LATHPDVQQK LQEEIDAVLP NKAPPTYDTV LQMEYLDMMV NETLRLFPVA MRLEVRCKKD VEINGVFIPK GVVVMIPSYA 400
dCYP3A26 301: IFIFAGYETT SSVLSFIMYE LATHPDVQQK LQEEIDAVLP NKAPPTYDTV LQMEYLDMMV NETLRLFPVA MRLEVRCKKD VEINGVFIPK GVVVMIPSYA 400
dCYP3A98 301: IFIFAGYETT SSVLSFIMYE LATHPDVQQK LQEEIDAVLP NKAPPTYDTV LQMEYLDMMV NETLRLFPVA MRLEVRCKKD VEINGVFIPK GVVVMIPSYA 400
dCYP3A99 301: IFIFAGYETT SSVLSFIMYE LATHPDVQQK LQEEIDAVLP NKAPPTYDTV LQMEYLDMMV NETLRLFPVA MRLEVRCKKD VEINGVFIPK GVVVMIPSYA 400
*.*.*.*.* *.*.*.*.* *.*.*.*.* *.*.*.*.* *.*.*.*.* *.*.*.*.* *.*.*.*.* *.*.*.*.* *.*.*.*.* *.*.*.*.* *.*.*.*.*

SRS-5
hCYP3A4 401: LHRDPKYWTE PEKFLPERFS KKNKDNIDPY IYTPFGSGPR NCIGMRFALM NMKLALIRVL QNFSFKPCKE TQIPLKLSLG GLLQPEKPIV LKVESRDGTV 500
hCYP3A5 401: LHRDPKYWTE PEKFLPERFS KKNKDNIDPY IYTPFGSGPR NCIGMRFALM NMKLALIRVL QNFSFKPCKE TQIPLKLSLG GLLQPEKPIV LKVESRDGTV 500
hCYP3A7 401: LHRDPKYWTE PEKFLPERFS KKNKDNIDPY IYTPFGSGPR NCIGMRFALM NMKLALIRVL QNFSFKPCKE TQIPLKLSLG GLLQPEKPIV LKVESRDGTV 500
hCYP3A43 401: LHRDPKYWTE PEKFLPERFS KKNKDNIDPY IYTPFGSGPR NCIGMRFALM NMKLALIRVL QNFSFKPCKE TQIPLKLSLG GLLQPEKPIV LKVESRDGTV 500
dCYP3A12 401: LHRDPKYWTE PEKFLPERFS KKNKDNIDPY IYTPFGSGPR NCIGMRFALM NMKLALIRVL QNFSFKPCKE TQIPLKLSLG GLLQPEKPIV LKVESRDGTV 500
dCYP3A26 401: LHRDPKYWTE PEKFLPERFS KKNKDNIDPY IYTPFGSGPR NCIGMRFALM NMKLALIRVL QNFSFKPCKE TQIPLKLSLG GLLQPEKPIV LKVESRDGTV 500
dCYP3A98 401: LHRDPKYWTE PEKFLPERFS KKNKDNIDPY IYTPFGSGPR NCIGMRFALM NMKLALIRVL QNFSFKPCKE TQIPLKLSLG GLLQPEKPIV LKVESRDGTV 500
dCYP3A99 401: LHRDPKYWTE PEKFLPERFS KKNKDNIDPY IYTPFGSGPR NCIGMRFALM NMKLALIRVL QNFSFKPCKE TQIPLKLSLG GLLQPEKPIV LKVESRDGTV 500
*.*.*.*.* *.*.*.*.* *.*.*.*.* *.*.*.*.* *.*.*.*.* *.*.*.*.* *.*.*.*.* *.*.*.*.* *.*.*.*.* *.*.*.*.* *.*.*.*.*

SRS-6
hCYP3A4 501: SGA 503
hCYP3A5 501: SGE 502
hCYP3A7 501: SGA 503
hCYP3A43 501: SGP 503
dCYP3A12 501: NGA 503
dCYP3A26 501: SGA 503
dCYP3A98 501: NGA 503
dCYP3A99 501: RGA 503
*.*.*.*.*
    
```

**Fig. 2**

DMD Fast Forward. Published on June 30, 2022 as DOI: 10.1124/dmd.121.000749  
This article has not been copyedited and formatted. The final version may differ from this version.

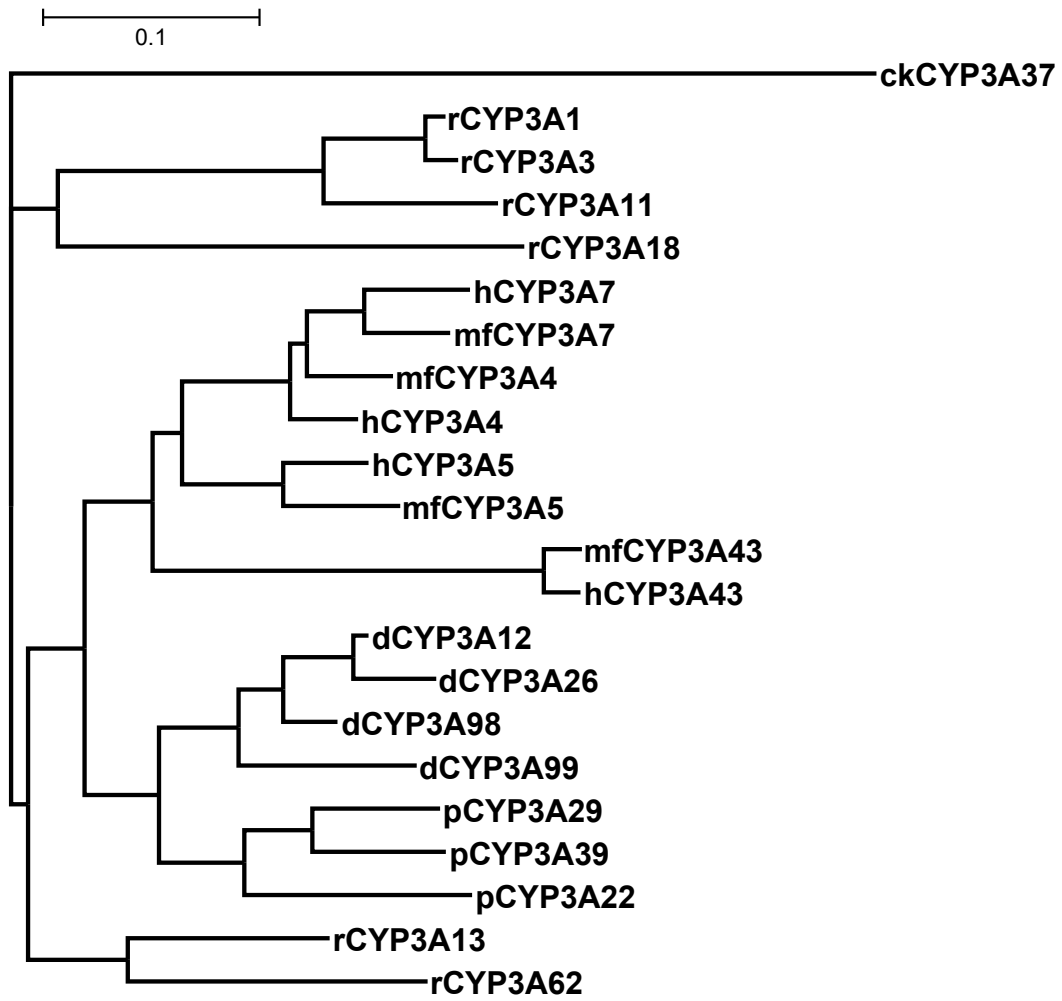


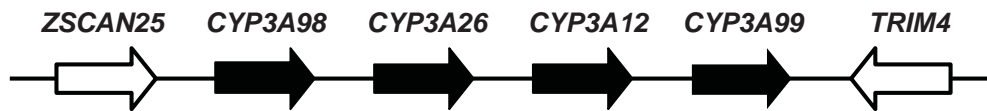


Fig. 3

**Human chromosome 7**



**Dog chromosome 6**



**Fig. 4**

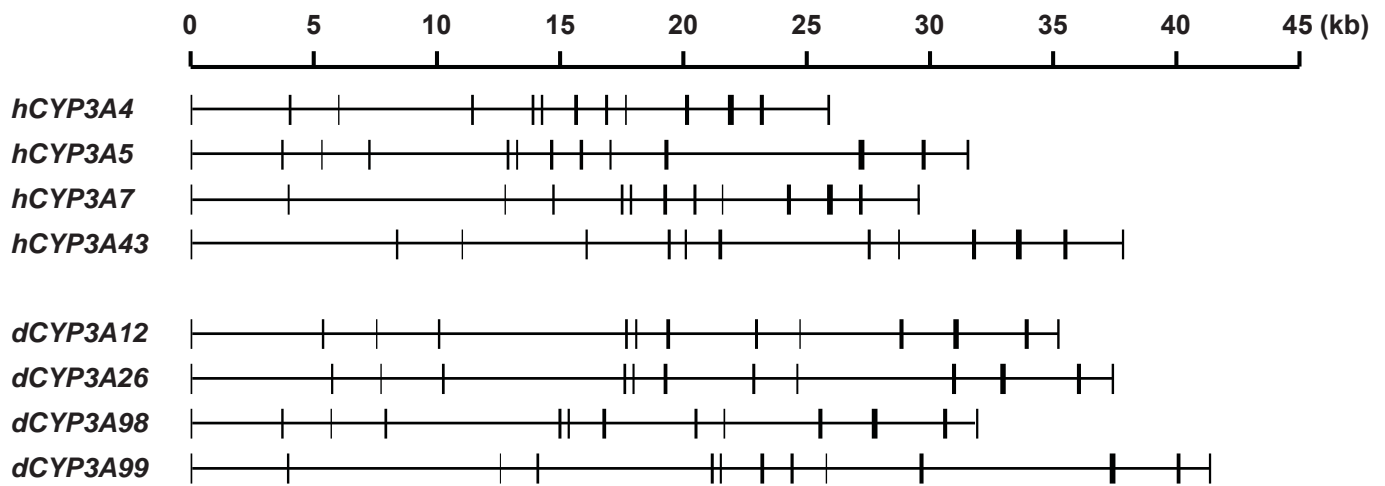


**Fig. 5**

DMD Fast Forward. Published on June 30, 2022 as DOI: 10.1124/dmd.121.000749  
This article has not been copyedited and formatted. The final version may differ from this version.

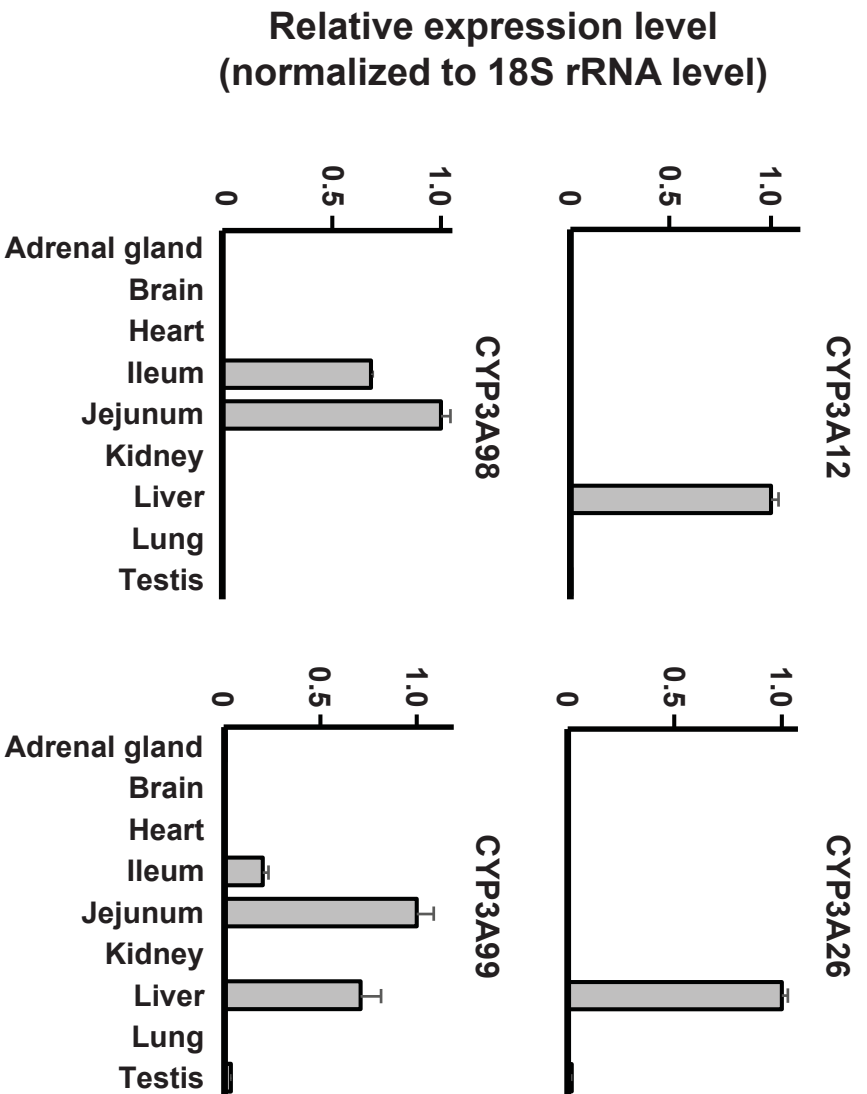


Fig. 6

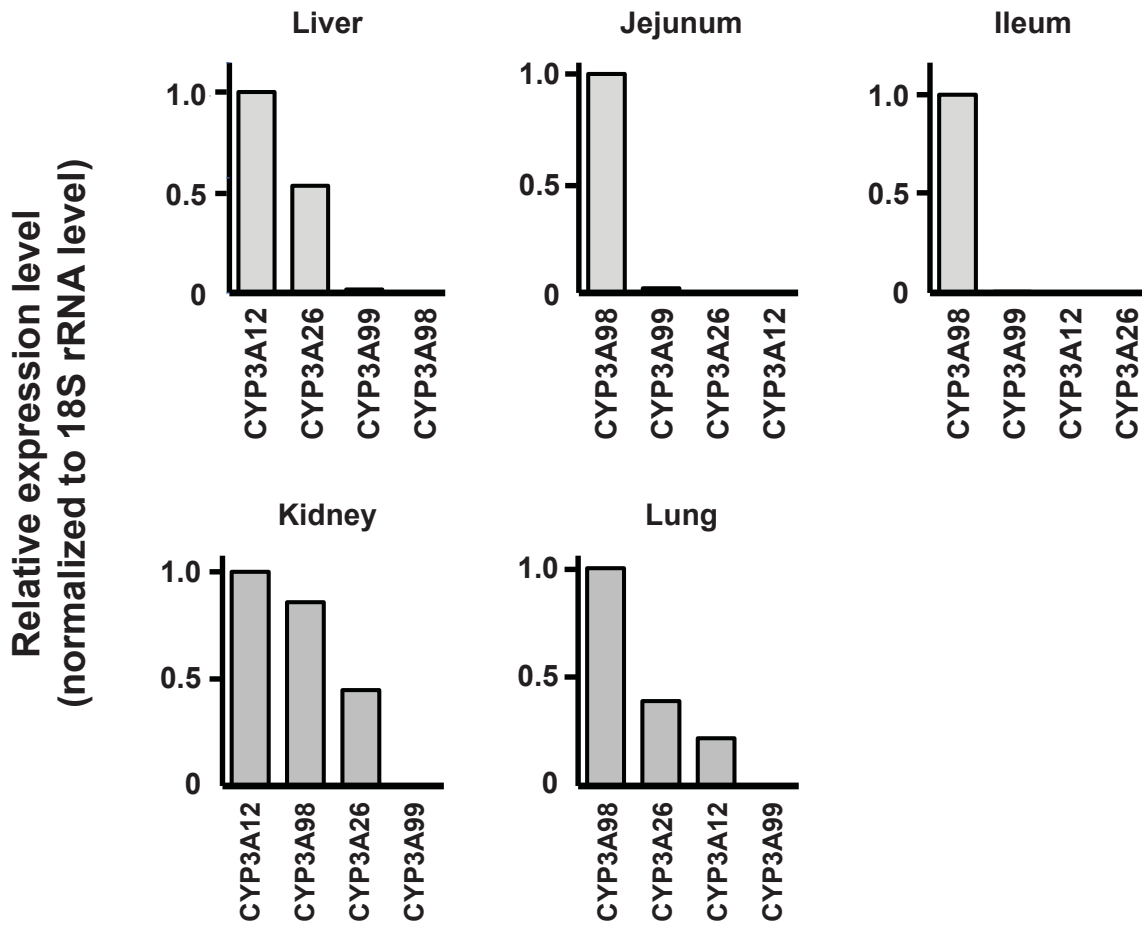
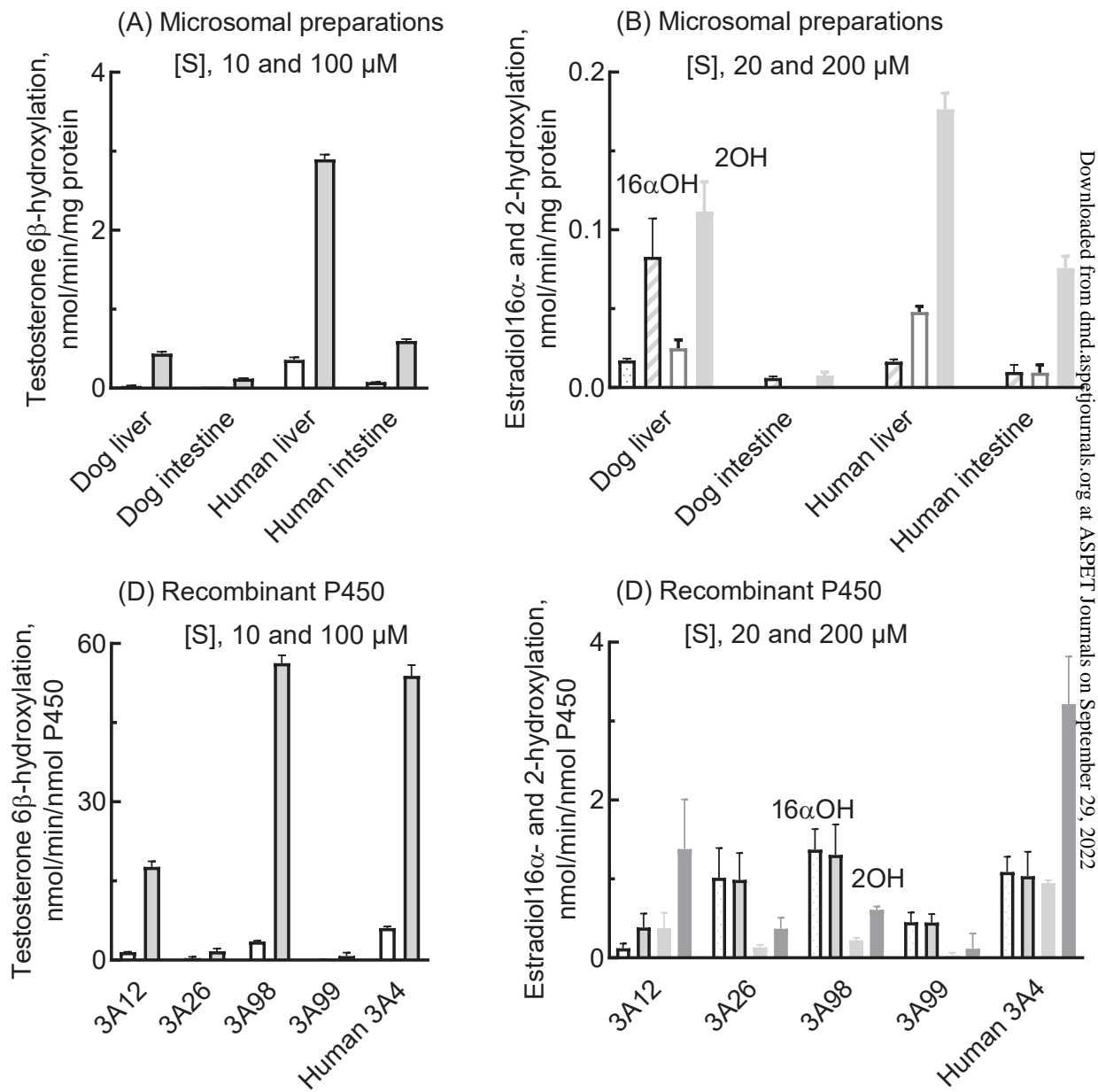
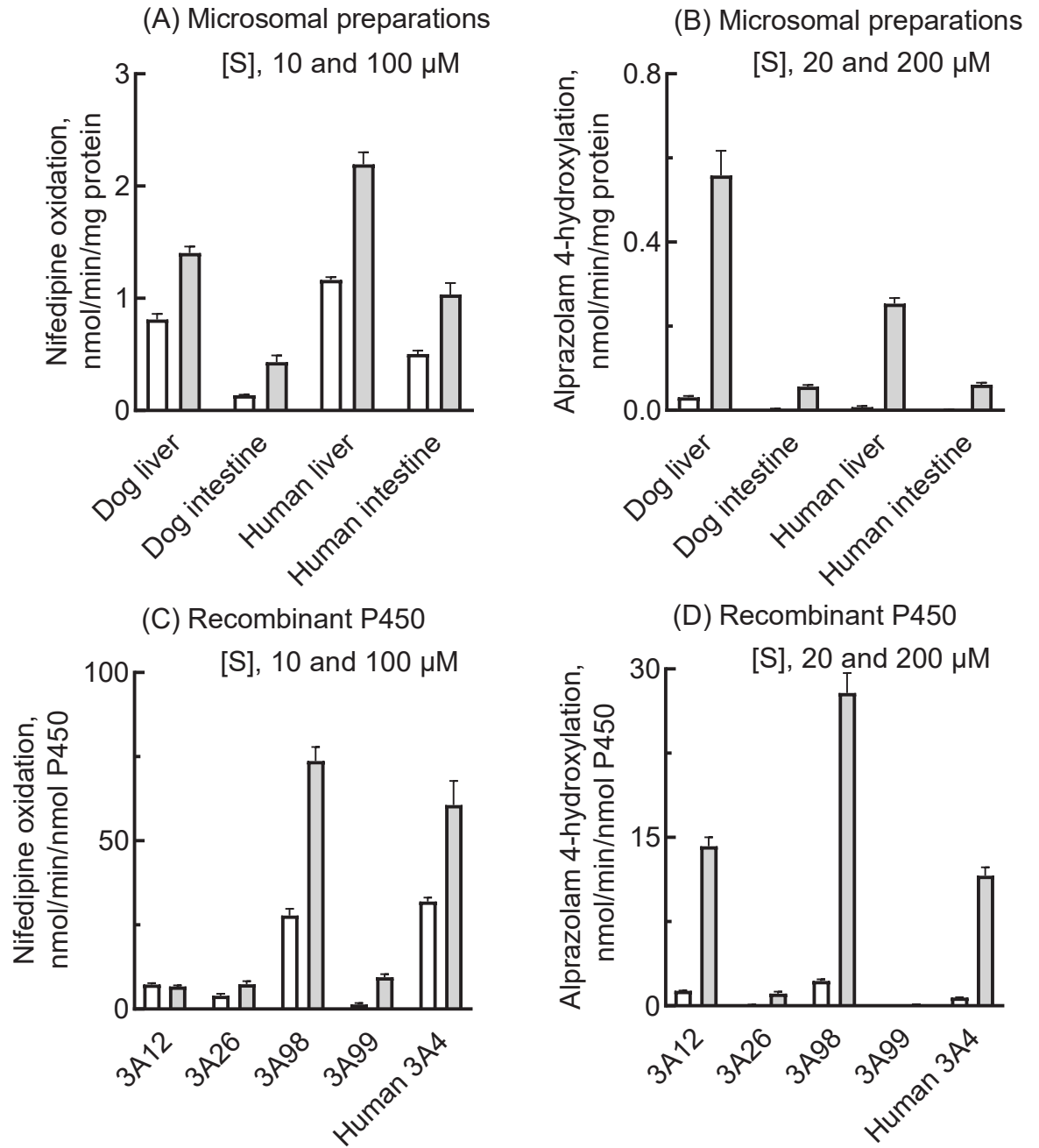


Fig.7



**Fig.8**



**Fig.9**

